KERNFORSCHUNGSZENTRUM

KARLSRUHE

April 1971

KFK 1411

Institut für Angewandte Kernphysik

Energy Levels of ^{98}Mo Excited in the (n,γ) Reaction

D. Heck, U. Fanger, W. Michaelis, H. Ottmar, H. Schmidt

GESELLSCHAFT FÜR KERNFORSCHUNG M.B.H.

KARLSRUHE

1.E.1:
3.A

Nuclear Physics A165 (1971) 327—352; © North-Holland Publishing Co., Amsterdam

ENERGY LEVELS OF ^{98}Mo EXCITED IN THE (n, γ) REACTION

D. HECK, U. FANGER, W. MICHAELIS, H. OTTMAR and H. SCHMIDT
Institut für Angewandte Kernphysik,
Kernforschungszentrum Karlsruhe, Karlsruhe, Germany

Received 17 December 1970

Abstract: The γ-ray spectra following thermal neutron capture in ^{97}Mo have been studied using Ge(Li) and NaI(Tl) detectors in various arrangements at the Karlsruhe research reactor FR-2. The target consisting of metallic molybdenum powder enriched to 92.8 % in ^{97}Mo was irradiated in external beam geometry. Energies and intensities of 247 transitions in the energy range 0.15 to 2.30 MeV and 4.9 to 8.7 MeV have been determined. Coincidence relationships measured with a Ge(Li)-Ge(Li) coincidence set-up were of considerable aid in constructing a level scheme for ^{98}Mo, which includes 29 excited states and 99 transitions. The analysis of angular correlation measurements of five cascades yielded the spin values of the levels involved in these cascades and the multipole mixtures of the linking transitions. The insufficiency of existing shell-model predictions for Mo isotopes is pointed out. Analogies with the properties of some states in the neighbouring ^{96}Mo isotope, as recently investigated by the present authors, are found. The discussion of the deduced levels in terms of a new collective model leads to the interpretation of ^{98}Mo as a nucleus in the transition region between vibrating spherical and rotating deformed nuclei.

E | NUCLEAR REACTIONS ^{97}Mo(n,γ), E = th; measured E_γ, I_γ, $\gamma\gamma$-coin, $\gamma\gamma(\theta)$, Q. ^{98}Mo deduced levels, J, π, δ. Enriched target, Ge(Li) and NaI(Tl) detectors.

1. Introduction

The level scheme of ^{98}Mo shows the rare phenomenon that the first excited level has spin and parity $J^\pi = 0^+$ [ref. [1])]. Among the six hitherto known nuclei with this property, ^{16}O, ^{40}Ca, ^{72}Ge, ^{90}Zr, ^{96}Zr and ^{98}Mo, the last nucleus is the only one, the excited states of which may be studied in the (n, γ) reaction. Earlier investigations of the level structure of ^{98}Mo have made use of inelastic deuteron scattering [2]), Coulomb excitation [3-7]), and the ^{97}Mo(d, p)^{98}Mo reaction [8-10]). In recently published papers results of the (n, n'γ) reaction [11]) and of the (p, p') reaction [12]) are reported. An attempt to clarify the structure of the low-lying $J^\pi = 0^+$ state has been made via the ^{98}Mo(p, p'e$^-$) reaction [13]).

In radioactive decay ^{98}Nb ($Q \approx 4.6$ MeV, $T_{\frac{1}{2}} = 52$ min, $J^\pi = 4^-$ or 5^-) and its short-lived isomer ($Q \approx 4.8$ MeV, $T_{\frac{1}{2}} = 2.8$ sec, $J^\pi = 1^+$) are the parent nuclei of ^{98}Mo [refs. [1,14-20])]. In an earlier study of the ^{97}Mo(n, γ) reaction only a list of the observed γ-rays was published [21,22]), but no level scheme has been deduced from the data. Therefore it seemed reasonable to reinvestigate this reaction †.

† Preliminary results of our investigation have been given in ref. [23]).

According to the assignment $J^\pi = \frac{5}{2}^+$ to the ground state of ^{97}Mo the neutron capture state in ^{98}Mo has $J^\pi = 2^+$ or 3^+. Therefore the levels directly fed from the capture state by dipole radiation may have spin values between $J = 1$ and 4. Thus at least part of the states should correspond to levels populated in the β-decay of ^{98}Nb or its short-lived isomer.

2. Experimental procedure

Thermal neutron beams from the Karlsruhe research reactor FR-2 were used to irradiate the sample consisting of 847 mg metallic molybdenum powder with high enrichment in ^{97}Mo. The abundance of the isotopes and their capture contributions are listed in table 1. Impurities of other elements are negligible as can be estimated from the spectrochemical analysis performed by the manufacturers. Details on the neutron beams may be taken from ref. [25]).

TABLE 1

Isotopic abundance of natural molybdenum and of the sample used in the present study

Isotope	σ (b) [a])	Natural Mo abundance % [a])	Natural Mo capture contribution % [a])	Enriched sample abundance % [b])	Enriched sample capture contribution %
92	< 0.3	15.84	< 1.5	0.27	< 0.04
94		9.04		0.24	
95	14.5	15.72	≈ 80	0.68	4.55
96	1.2	16.53	7	1.69	0.94
97	2.2	9.46	8	92.8	94.17
98	0.15	23.78	4	3.97	0.27
100	0.20	9.63	0.7	0.37	0.034

[a]) Ref. [24]).

[b]) Analysis of the manufacturers AERE, Harwell, Berkshire, England and Union Carbide Corporation, ORNL, Tennessee, USA.

For the measurement of the γ-rays four devices were used: (i) An anti-Compton arrangement [26]) with a 4.9 cm^3 Ge(Li) diode for the energy range 0.15 to 2.30 MeV. The energy resolution of this instrument amounted to 1.62 keV FWHM for the 662 keV ^{137}Cs γ-ray. (ii) A double-escape spectrometer for energies above 4.9 MeV with a planar Ge(Li) diode of 2.3 cm^3 active volume. A resolution of 5.4 keV FWHM was found for the double-escape peaks of the ^{57}Fe doublet at 7.6 MeV. (iii) A coincidence arrangement [27]) consisting of two Ge(Li) detectors with about 30 cm^3 volume and (iv) a $\gamma\gamma$ angular correlation apparatus [28,29]) with two 10.2 cm ⌀ × 12.7 cm NaI(Tl) crystals. The latter two instruments were coupled to the Karlsruhe data acquisition system MIDAS [30,31]). Details of the energy and intensity calibration, coincidence and angular correlation analysis may be found in our recent publication[32]) on the ^{95}Mo(n, γ)^{96}Mo reaction.

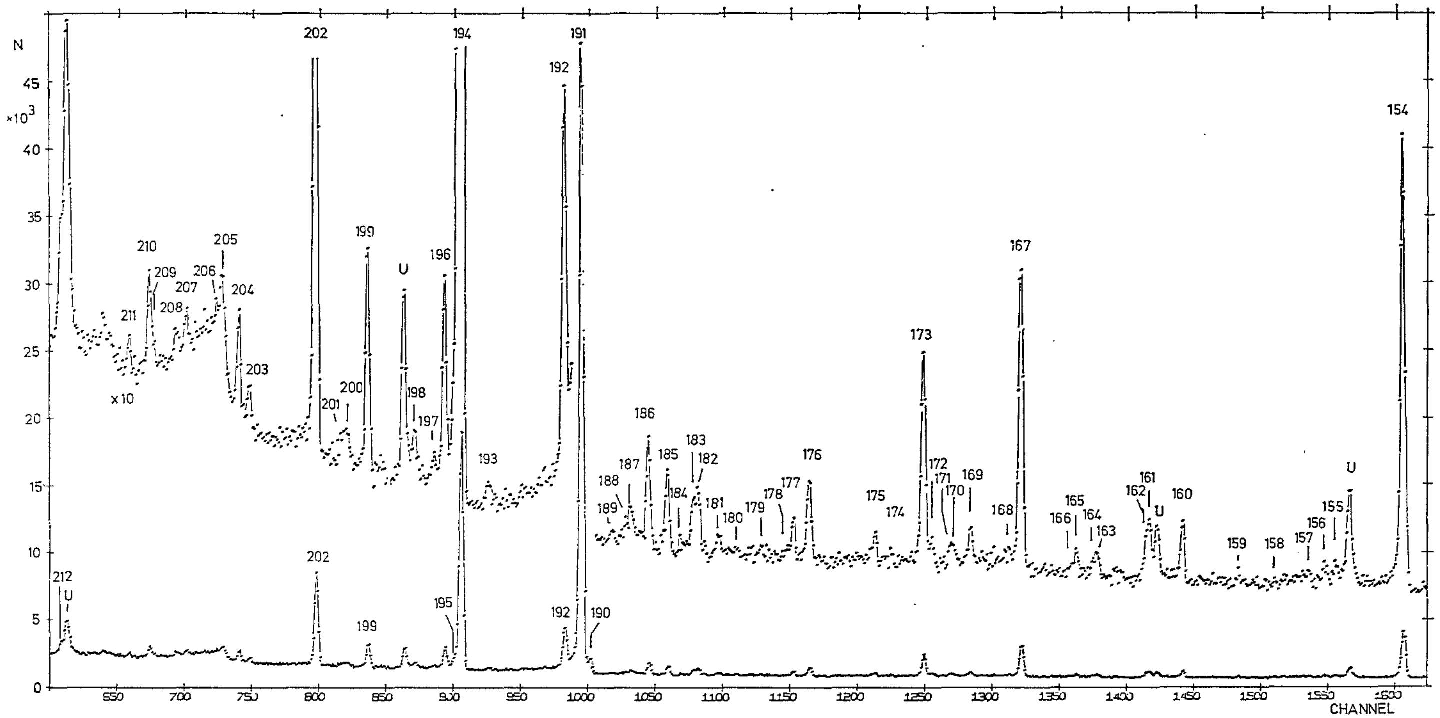

Fig. 1. Portion of the neutron capture γ-ray spectrum as observed with the anti-Compton spectrometer, energy range 500 to 1240 keV. The numbers assigned to the peaks correspond to those of table 2. U denotes background peaks.

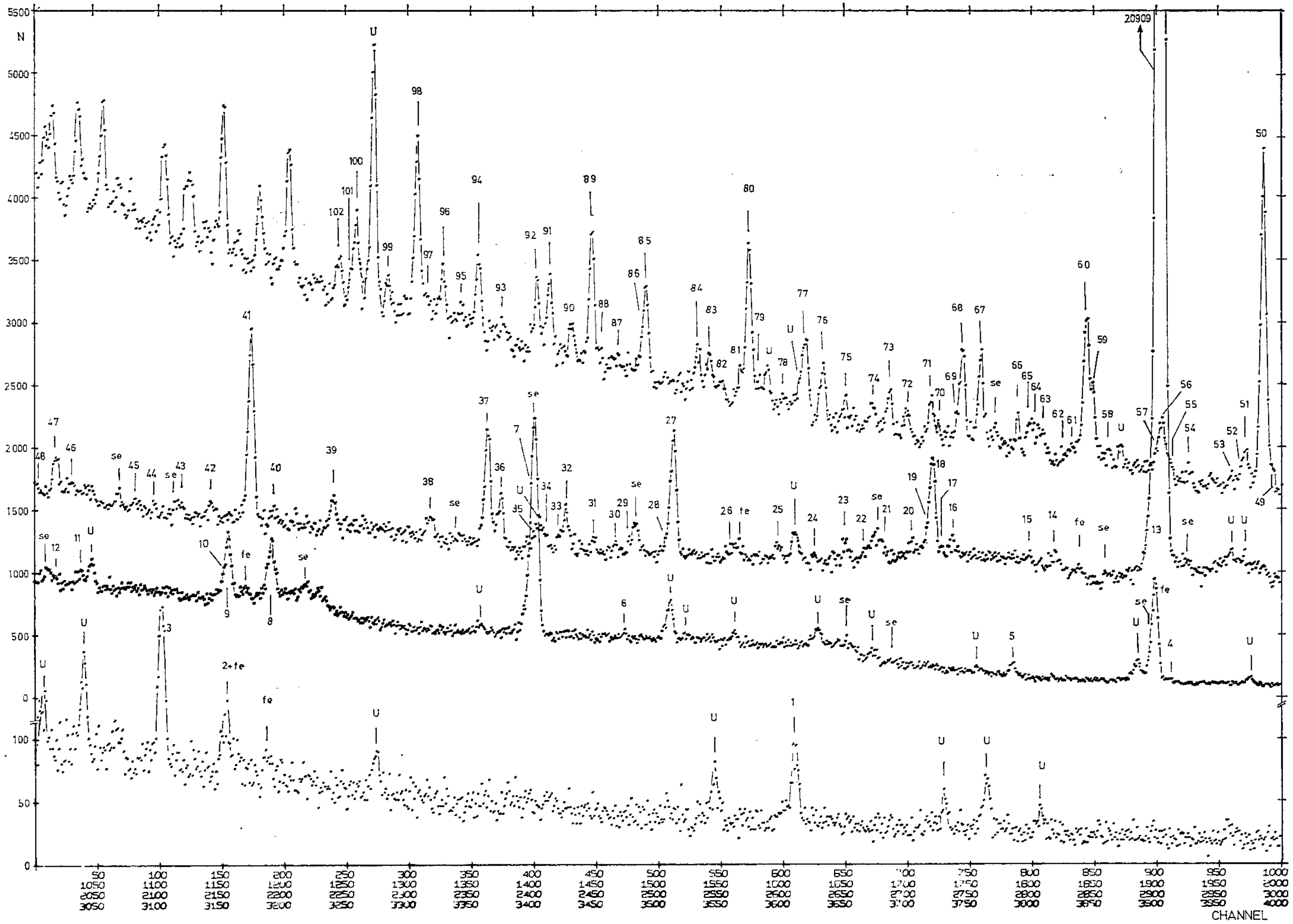

Fig. 2. Single γ-ray spectrum of ^{98}Mo in the energy range 4.7 to 8.7 MeV as observed with a planar diode. The numbers assigned to the peaks correspond with those of table 2. The symbols U, se and fe denote background, single-escape and full-energy peaks.

TABLE 2

Gamma rays from the reaction $^{97}Mo(n, \gamma)^{98}Mo$

Line no.	Energy E_γ(keV)	Error ΔE_γ(keV)	Intensity [a]) I_γ	Error [b]) ΔI_γ	Assignment [c])
1	8375.8	0.8	0.05	0.01	$^{95}Mo(n, \gamma)$
2	7907.4	0.8	0.025	0.01	C–735
3	7854.6	0.6	0.10	0.01	C–787
4	7657.9	1.3	0.015	0.01	$^{95}Mo(n, \gamma)$
5	7528.6	0.8	0.07	0.01	$^{95}Mo(n, \gamma)$
6	7208.8	1.1	0.025	0.01	C–1432
7	7132.5	0.6	0.32	0.05	C–1510
8	6919.1	0.6	0.25	0.015	$^{95}Mo(n, \gamma)$
9	6883.5	0.6	0.25	0.02	C–1759
10	6878.9	2.3	0.02	0.015	u
11	6760.7	0.7	0.055	0.01	C–1881
12	6740.1	1.4	0.02	0.01	u
13	6624.6	0.6	10.0		C–2018
14	6536.9	0.7	0.065	0.01	C–2105
15	6514.9	1.0	0.025	0.01	
16	6451.7	0.7	0.055	0.01	
17	6443.3	2.0	0.015	0.01	u
18	6435.6	0.6	0.37	0.03	C–2207
19	6430.7	1.1	0.035	0.015	
20	6418.5	0.7	0.045	0.01	C–2224
21	6392.6	0.7	0.075	0.015	
22	6380.8	1.3	0.03	0.015	
23	6364.0	0.6	0.07	0.015	$^{95}Mo(n, \gamma)$
24	6338.5	1.0	0.025	0.01	
25	6308.4	0.5	0.055	0.01	C–2333
26	6270.4	0.9	0.04	0.01	
27	6222.7	0.5	0.41	0.03	C–2420
28	6218.9	1.0	0.05	0.02	
29	6186.5	1.5	0.025	0.015	u
30	6174.2	1.0	0.025	0.01	
31	6156.7	0.7	0.04	0.01	C–2485
32	6134.1	0.5	0.13	0.01	
33	6128.2	0.7	0.045	0.01	$^{95}Mo(n, \gamma)$
34	6116.0	0.7	0.06	0.01	
35	6102.2	1.0	0.03	0.01	u
36	6080.0	0.6	0.17	0.02	C–2562
37	6069.4	0.6	0.39	0.03	C–2573
38	6021.9	0.7	0.08	0.01	C–2621
39	5941.9	0.8	0.075	0.02	C–2701
40	5893.2	0.8	0.04	0.01	
41	5874.5	0.6	0.58	0.05	C–2768
42	5841.8	0.7	0.045	0.01	
43	5817.2	1.0	0.03	0.01	
44	5794.5	0.9	0.02	0.01	u
45	5778.8	0.7	0.035	0.01	
46	5725.8	0.8	0.025	0.01	
47	5713.3	0.7	0.11	0.01	$^{95}Mo(n, \gamma)$
48	5697.0	1.5	0.025	0.015	u
49	5686.5	0.7	0.065	0.015	

TABLE 2 (continued)

Line no.	Energy E_γ(keV)	Error ΔE_γ(keV)	Intensity [a]) I_γ	Error [b]) ΔI_γ	Assignment [c])
50	5680.0	0.6	0.99	0.08	C–2962
51	5665.0	0.7	0.10	0.03	C–2977
52	5661.2	1.6	0.04	0.03	u
53	5652.8	1.1	0.03	0.015	
54	5618.6	0.7	0.035	0.01	
55	5601.8	0.6	0.055	0.01	^{95}Mo(n, γ)
56	5596.3	0.6	0.15	0.02	C–3046
57	5592.1	0.7	0.055	0.02	
58	5551.7	0.7	0.035	0.01	
59	5538.8	0.6	0.20	0.02	C–3103
60	5533.4	0.8	0.33	0.05	C–3109
61	5527.1	0.9	0.035	0.01	
62	5520.6	0.9	0.03	0.01	u
63	5497.9	0.7	0.065	0.02	
64	5493.3	1.0	0.035	0.02	u
65	5487.0	0.5	0.10	0.02	C–3156
66	5476.4	0.5	0.075	0.01	
67	5446.4	0.4	0.24	0.02	C–3196
68	5431.5	0.4	0.25	0.02	C–3211
69	5426.9	1.0	0.045	0.02	
70	5411.0	1.0	0.03	0.01	u
71	5405.3	0.5	0.10	0.01	
72	5385.2	0.5	0.065	0.01	
73	5370.9	0.4	0.11	0.01	
74	5356.8	0.5	0.07	0.01	
75	5333.7	0.8	0.035	0.01	
76	5316.1	0.4	0.14	0.015	
77	5302.0	0.4	0.20	0.03	
78	5283.7	0.8	0.035	0.015	u
79	5262.3	0.6	0.055	0.01	
80	5255.1	0.4	0.43	0.04	
81	5248.5	0.6	0.06	0.015	50 % ^{95}Mo(n, γ)
82	5231.7	0.7	0.045	0.01	
83	5222.3	0.4	0.11	0.01	
84	5212.8	0.4	0.11	0.01	
85	5170.0	0.4	0.23	0.02	
86	5165.8	1.1	0.04	0.02	u
87	5146.2	1.0	0.03	0.02	u
88	5132.2	0.8	0.02	0.015	u
89	5125.5	0.4	0.34	0.03	
90	5108.6	0.5	0.085	0.01	
91	5090.6	0.4	0.20	0.02	
92	5080.3	0.4	0.18	0.02	
93	5052.1	0.7	0.05	0.02	
94	5031.9	0.4	0.20	0.02	
95	5017.6	0.7	0.05	0.02	
96	5002.5	0.4	0.13	0.02	
97	4988.4	0.6	0.06	0.02	
98	4981.5	0.4	0.44	0.04	
99	4957.2	0.6	0.07	0.02	

TABLE 2 (continued)

Line no.	Energy E_γ(keV)	Error ΔE_γ(keV)	Intensity [a]) I_γ	Error [b]) ΔI_γ	Assignment [c])
100	4931.3	0.5	0.20	0.03	
101	4927.3	1.1	0.05	0.03	
102	4916.8	0.5	0.10	0.02	
					Note: As to the intensities after this point see comments in the text (subsect. 3.1)
103	2280.5	0.3	0.26	0.10	
104	2258.7	0.4	0.21	0.10	3046–787
105	2176.0	0.3	0.40	0.10	
106	2082.3	0.2	0.66	0.15	
107	2017.4	0.2	1.88	0.20	2018– 0
108	1979.9	0.3	0.64	0.15	2768–787
109	1945.1	0.4	0.37	0.10	
110	1913.1	0.3	0.50	0.10	2701–787
111	1886.3	0.7	0.22	0.10	2621–735
112	1869.4	0.4	0.37	0.10	
113	1847.9	0.7	0.31	0.15	
114	1833.0	0.3	0.55	0.10	2621–787
115	1785.4	0.3	0.69	0.15	2573–787
116	1774.7	0.2	1.40	0.15	2562–787
117	1758.9	0.5	0.26	0.10	1759– 0
118	1748.0	0.6	0.23	0.10	
119	1739.3	0.4	0.32	0.10	
120	1701.8	0.3	0.48	0.10	
121	1698.0	0.3	0.50	0.10	2485–787
122	1690.5	0.6	0.20	0.10	
123	1643.2	0.8	0.14	0.10	u
124	1631.4	0.2	0.86	0.10	
125	1612.5	0.4	0.28	0.10	
126	1598.8	0.7	0.16	0.10	3109–1510
127	1555.4	0.5	0.16	0.10	
128	1545.95	0.12	2.40	0.20	2333–787
129	1541.6	0.3	0.33	0.10	
130	1512.0	0.3	0.32	0.10	
131	1508.0	0.5	0.19	0.10	
132	1497.9	0.4	0.26	0.10	$^{95}Mo(n,\gamma)$
133	1472.9	1.0	0.08	0.10	u
134	1467.1	0.3	0.36	0.10	2977–1510
135	1452.3	0.3	0.34	0.10	2962–1510
136	1447.6	0.6	0.13	0.10	u
137	1436.6	0.3	0.46	0.10	2224–787
138	1432.31	0.11	4.87	0.40	1432– 0
139	1419.39	0.13	1.57	0.15	2207–787
140	1406.3	0.8	0.11	0.10	u
141	1394.2	0.2	0.44	0.10	
142	1388.0	0.3	0.27	0.10	
143	1370.1	0.2	0.52	0.10	2105–735
144	1359.7	0.5	0.19	0.10	
145	1348.4	0.6	0.15	0.10	

TABLE 2 (continued)

Line no.	Energy E_{γ}(keV)	Error ΔE_{γ}(keV)	Intensity [a]) I_{γ}	Error [b]) ΔI_{γ}	Assignment [c])
146	1323.9	0.4	0.21	0.10	
147	1317.40	0.12	1.94	0.30	2105–787, 10 % ^{95}Mo(n, γ)
148	1287.2	0.3	0.48	0.15	3046–1759
149	1285.42	0.14	1.36	0.15	2796–1510
150	1259.8	0.4	0.17	0.10	
151	1254.6	0.3	0.19	0.10	u
152	1249.9	0.2	0.26	0.10	
153	1241.2	0.4	0.14	0.10	
154	1230.23	0.12	9.77	0.90	2018–787
155	1193.3	0.3	0.35	0.10	3211–2018
156	1187.6	0.3	0.27	0.10	
157	1178.1	0.5	0.23	0.10	3196–2018
158	1155.8	0.8	0.12	0.10	u
159	1140.8	0.4	0.22	0.10	2573–1432
160	1110.81	0.14	0.94	0.10	2621–1510
161	1093.2	0.2	0.82	0.10	1881–787
162	1091.2	0.2	0.68	0.10	3109–2018, 50 % ^{95}Mo(n, γ)
163	1064.4	0.3	0.36	0.10	
164	1062.2	0.3	0.20	0.10	
165	1053.1	0.3	0.37	0.10	2485–1432
166	1050.8	0.4	0.12	0.10	3156–2105
167	1023.60	0.11	4.78	0.40	1759–735
168	1017.1	0.5	0.19	0.10	
169	996.1	0.2	0.49	0.10	2506–1510
170	987.6	0.5	0.21	0.10	2420–1432
171	985.5	0.4	0.25	0.10	
172	974.9	0.3	0.30	0.10	2485–1510
173	971.01	0.11	2.89	0.30	1759–787
174	952.7	0.9	0.09	0.10	u
175	944.7	0.2	0.40	0.10	2962–2018
176	909.59	0.13	1.07	0.10	2420–1510
177	900.9	0.2	0.43	0.10	2333–1432
178	897.5	0.7	0.08	0.10	u
179	883.8	0.4	0.14	0.10	
180	866.6	0.5	0.11	0.10	3211–2344
181	860.8	0.2	0.25	0.10	
182	849.9	0.3	0.65	0.10	^{95}Mo(n, γ)
183	847.4	0.3	0.56	0.10	^{95}Mo(n, γ)
184	840.4	0.8	0.08	0.10	u
185	833.61	0.13	0.82	0.10	2344–1510
186	823.44	0.12	1.09	0.10	2333–1510
187	814.2	0.2	0.43	0.10	2573–1759
188	811.5	0.5	0.17	0.10	3156–2344, 20 % ^{95}Mo(n, γ)
189	803.6	0.5	0.11	0.10	2562–1759
190	791.5	0.2	1.24	0.15	2224–1432
191	787.42	0.10	62.0	5.0	787–0
192	778.30	0.14	3.69	0.25	^{95}Mo(n, γ)

TABLE 2 (continued)

Line no.	Energy E_γ(keV)	Error ΔE_γ(keV)	Intensity [a]) I_γ	Error [b]) ΔI_γ	Assignment [c])
193	737.4	0.6	0.20	0.10	^{95}Mo(n, γ)
194	722.70	0.10	19.0	1.6	1510–787
195	719.7	0.2	0.66	0.10	^{95}Mo(n, γ)
196	713.88	0.15	1.60	0.20	2224–1510
197	708.2	0.5	0.12	0.10	
198	697.6	0.2	0.34	0.10	1432–735
199	672.63	0.11	1.57	0.15	2105–1432
200	661.5	0.5	0.20	0.10	2420–1759
201	659.1	0.3	0.19	0.10	
202	644.89	0.11	5.78	0.50	1432–787
203	608.8	0.2	0.23	0.05	^{95}Mo(n, γ)
204	603.33	0.12	0.59	0.05	2621–2018
205	594.6	0.3	0.39	0.15	2105–1510
206	591.5	0.3	0.18	0.15	^{95}Mo(n, γ)
207	575.0	0.2	0.17	0.05	2333–1759
208	569.9	0.3	0.16	0.05	
209	557.1	0.4	0.16	0.10	2977–2420
210	555.4	0.2	0.41	0.05	2573–2018
211	545.0	0.2	0.18	0.05	2562–2018
212	507.8	0.2	0.40	0.05	2018–1510
213	500.5	0.3	0.10	0.03	
214	493.4	0.6	0.04	0.03	2701–2207
215	490.3	0.5	0.05	0.05	u
216	458.7	0.3	0.08	0.03	
217	455.1	0.3	0.06	0.03	3156–2701
218	449.1	0.3	0.07	0.03	1881–1432
219	446.99	0.13	0.29	0.03	
220	434.5	0.2	0.16	0.03	2768–2333
221	411.4	0.2	0.22	0.03	
222	402.2	0.2	0.09	0.03	2420–2018
223	399.88	0.15	0.20	0.03	3196–2796
224	386.3	0.8	0.03	0.03	u
225	380.48	0.14	0.15	0.03	2485–2105
226	368.6	0.7	0.05	0.03	^{95}Mo(n, γ)
227	365.2	0.4	0.04	0.03	
228	350.99	0.12	0.45	0.05	10 % ^{95}Mo(n, γ)
229	346.8	0.5	0.04	0.03	D
230	340.0	0.5	0.05	0.02	
231	335.4	0.2	0.07	0.02	3103–2768
232	326.21	0.12	0.30	0.03	1759–1432
233	319.3	0.4	0.33	0.03	
234	314.6	0.3	0.03	0.02	2420–2105
235	307.0	0.3	0.03	0.02	
236	298.2	0.3	0.05	0.02	D
237	286.9	0.3	0.05	0.02	
238	259.01	0.10	2.77	0.25	2018–1759
239	241.2	0.2	0.09	0.03	^{95}Mo(n, γ)
240	239.2	0.2	0.11	0.03	2573–2333
241	202.8	0.3	0.02	0.01	
242	195.6	0.5	0.07	0.02	

TABLE 2 (continued)

Line no.	Energy E_γ(keV)	Error ΔE_γ(keV)	Intensity [a]) I_γ	Error [b]) ΔI_γ	Assignment [c])
243	182.0	0.4	0.03	0.02	D
244	172.95	0.12	0.42	0.05	2506–2333
245	158.6	0.3	0.14	0.05	D
246	155.3	0.3	0.04	0.03	
247	152.2	0.4	0.05	0.03	2485–2333

Target: metallic molybdenum powder with enrichment of ^{97}Mo to 92.8 %.

[a]) The intensities have been normalized to that of line no. 13, the intensity of which has been adopted from ref. [33]) (cf. subsect. 3.1).

[b]) See text.

[c]) Transitions placed in the level scheme are denoted by the level energy values. The following abbreviations are used: C = capture state, D = possible doublet, u = uncertain line.

3. Results

3.1. SINGLES AND COINCIDENCE SPECTRA

Fig. 1 shows a portion of the anti-Compton spectrum between 500 and 1240 keV. The singles spectrum recorded with the planar diode in the energy range between 4.7 and 8.7 MeV is presented in fig. 2. The energy and intensity values as obtained from these devices are summarized in table 2. The errors quoted for the energies include statistical and systematic uncertainties. The presented intensities refer to the intensity of the 6625 keV γ-ray. The intensity scale of the energy range 0.15 to 2.30 keV is linked to the 6625 keV γ-ray intensity by the ^{96}Mo γ-rays observed at 6919 keV and 778 keV, the intensity ratio of which is well known from ref. [32]). The listed intensity errors originate from the statistical fluctuations and deviations of the adopted polynomial from the real efficiency function; also errors of the intensity ratio of the ^{96}Mo lines are taken into account. The absolute intensity value $I_{6625} = 10.0$ is derived from ref. [33]) considering the capture contribution of ^{97}Mo in natural molybdenum (cf. table 1).

By this normalization the intensity values of table 2 refer to 100 neutron capture events in ^{97}Mo with an error of 30 % at maximum, arising from uncertainties of capture cross sections and of the 6.63 MeV γ-ray intensity given in ref. [33]).

If a background line or, in the high-energy region, a single-escape or full-energy peak contributes to an observed peak, these contributions have been subtracted and the resulting uncertainties in energy and intensity are taken into account in table 2.

The results of the coincidence measurements are reproduced in the coincidence matrix of table 3. In this table uncertain coincidences are labelled with brackets. If the assignment of an observed peak to a certain transition is ambiguous, all the transitions in question are listed in column 1 of table 3. According to the selected energy range only coincidence relationships of transitions in the range 0.1 to 1.3 MeV with those in the range 0.55 to 1.55 MeV have been established.

TABLE 3

$\gamma\gamma$ coincidence relationships in ^{98}Mo, observed with two 30 cm^3 Ge(Li) detectors

Lines observed in coincidence spectra (keV)	Digital window setting (keV)												
	169–178	254–264	639–650	668–678	709–717	718–730	787–797	965–979	1017–1030	1222–1239	1280–1292	1426–1442	1537–1555
173						+	+						
196			+			+				+	+		
259							+	+	+				
326							+						
380							+						
400											+		
447							+						
508						+	+						
555							+			+			
575	+												
595						(+)							
603		+											
645		+		+			+						
673			+				+						
714						+	+						
723	+				+		+				+	(+)	
787	+	+	+	+	+	+		+		+	+	+	+
792			+				(+)					+	
823	+					+	+						
834						+	+						
910						+	+						
971		+					+						
1017							+						
1024		+											
1053			(+)										
1111						+	(+)						
1178		+								(+)			
1188, 1194							+						
1230							+						
1285					(+)	+	+						
1317							+						
1419							+						
1432, 1437				+			+						
1467						+							
1546	+						+						

Typical results of the coincidence measurements are the spectra coincident with the transitions 259 keV, 723 keV and 787 keV, which are presented in fig. 3. The inset in this figure shows the positions of the digital windows used for the subtraction of the coincident background under the peaks.

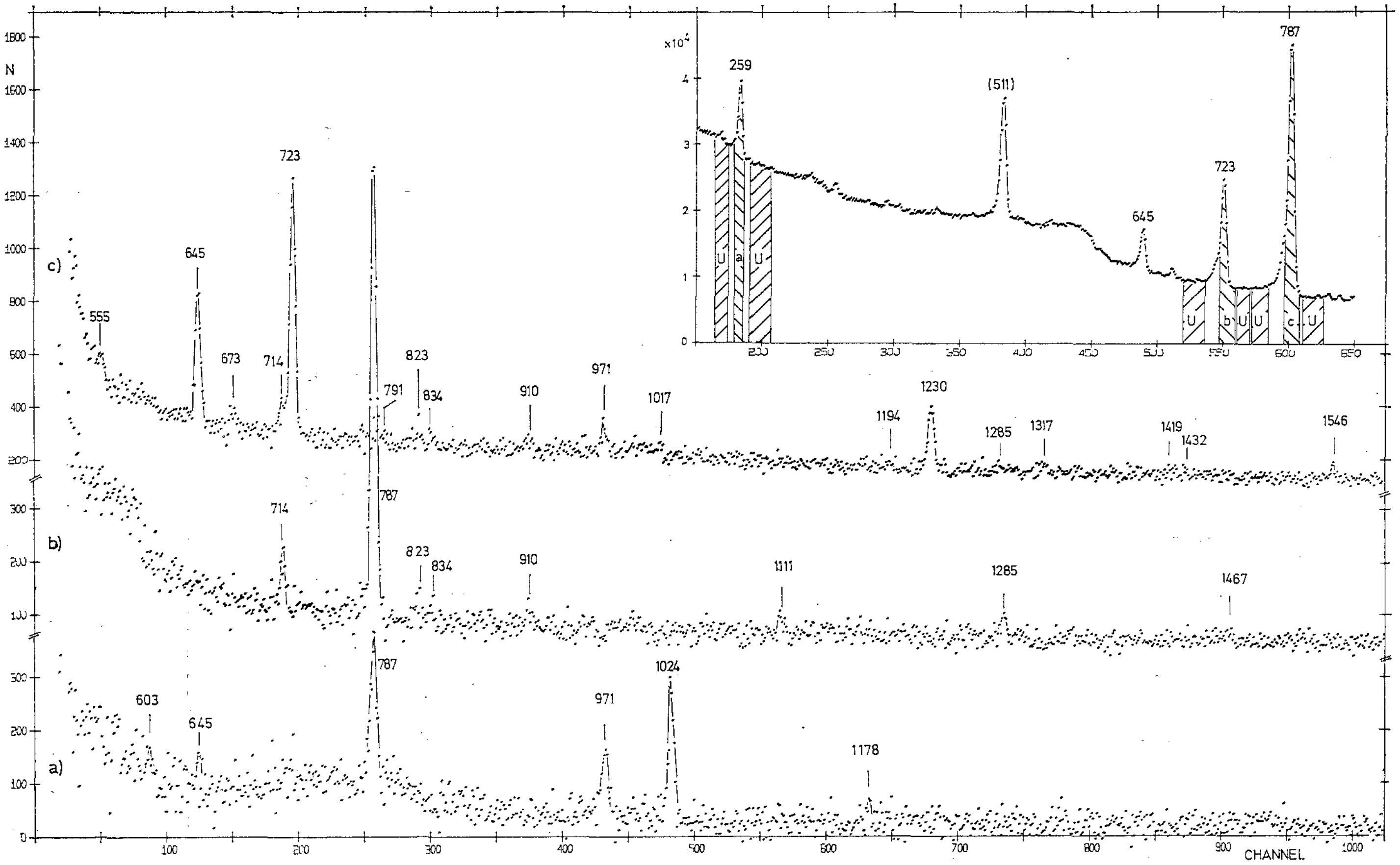

Fig. 3. γ-ray spectra of ^{98}Mo observed with two Ge(Li) detectors in the coincidence arrangement. The spectra are coincident with the γ-rays a) 259 keV, b) 723 keV and c) 787 keV. The positions of the digital coincidence and background (denoted with U) gates used in the background subtraction technique are shown in the inset.

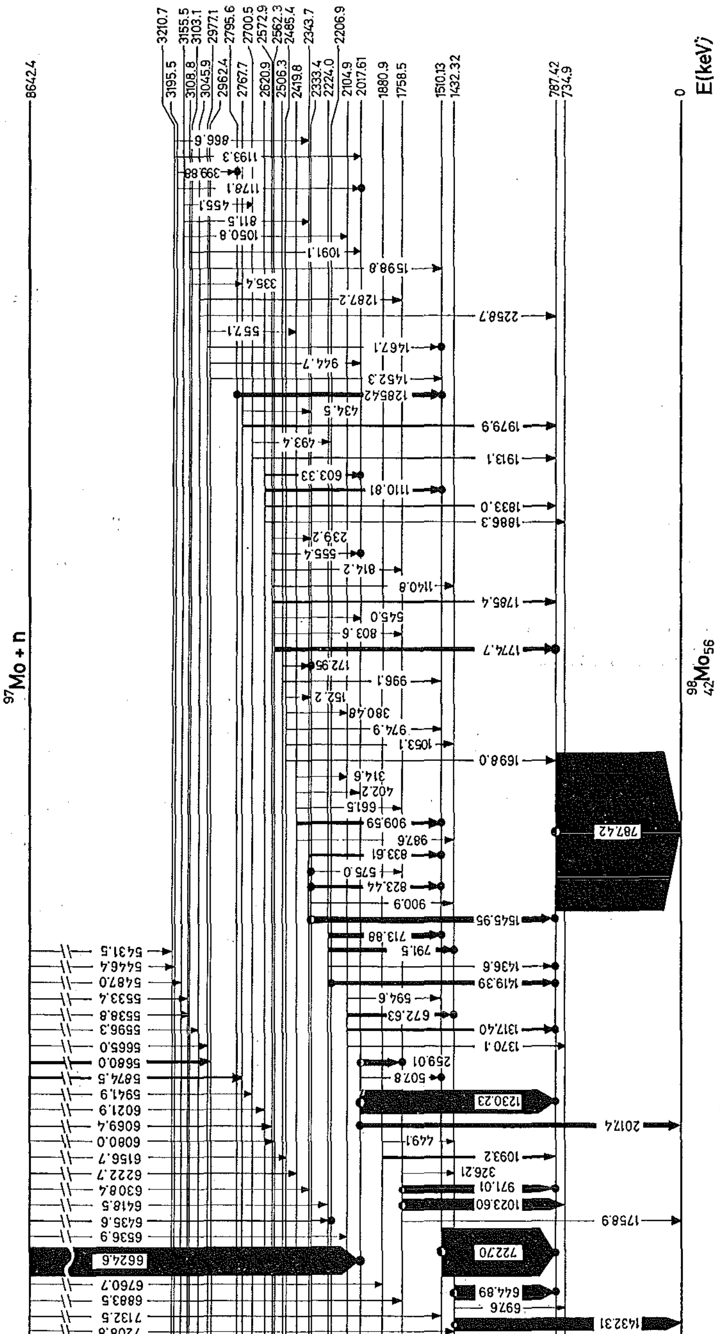

Fig. 4. Level scheme of ^{98}Mo deduced from the present (n, γ) study. Energies are quoted in keV. Observed coincidences are marked by dots. The arrow width gives a rough indication of the transition intensity.

With the NaI(Tl) detectors of the angular correlation apparatus [28,29] some coincidence relationships involving high-energy transitions have been observed. In coincidence with the intense primary transition at 6.62 keV we have found peaks at the following energies: 2.02 MeV, 1.43 MeV, 1.23 MeV, 1.02 MeV, 0.97 MeV, 0.79 MeV, 0.72 MeV and 0.64 MeV. The peaks at 1.43 MeV and 0.64 MeV and a fraction of the 0.72 MeV peak have to be attributed to the transitions at 7.21 MeV and 7.13 MeV, the single-escape peaks of which are partly covered by the coincidence gate. Peaks at 2.02 MeV, 1.43 MeV, 1.23 MeV, 0.79 MeV, 0.71 MeV and 0.64 MeV appear in coincidence with a gate at 6.43 MeV. The peaks at 2.02 MeV and 1.23 MeV are due to coincidences with the Compton edge of the 6.62 MeV transition which appears in the selected coincidence gate.

3.2. LEVEL SCHEME

In fig. 4 the level scheme of ^{98}Mo is presented as it is derived from the (n, γ) reaction. The levels are essentially based on observed coincidence relationships (indicated by dots) and on the presence of primary transitions proceeding from the capture state. The arrow width gives a rough indication of the transition intensity. For the computation of the level energies a computer program [34]) has been used. In this program the sums of the energies of all the de-exciting transitions (corrected for recoil) and of the levels at which these transitions arrive, are formed and the weighted mean value of these sums is taken as the level energy. (The energy of the 735 keV level has been determined from the energy values of the 1759 keV level and the 1024 keV transition.) The binding energy B_n of the last neutron in the ^{98}Mo nucleus is determined in the same manner. The weighted mean value is

$$B_n = 8642.4 \pm 0.5 \text{ keV}.$$

The uncertainty includes possible systematic errors from the calibration lines. The result is in excellent agreement with the value $B_n = 8642.2 \pm 3.6$ keV as derived from mass differences by Mattauch [35]).

3.3. ANGULAR CORRELATIONS

By analysis of the spectra recorded with the angular correlation apparatus the angular correlation function

$$W(\theta) = 1 + A_2 P_2(\cos\theta) + A_4 P_4(\cos\theta)$$

of the most intense cascades has been determined.

In fig. 5 the measured coefficients are displayed in the A_2, A_4 plane together with the theoretical coefficients for cascades with the spin sequence J-2-0 (J = 1, 2, 3 or 4). The ellipses are labelled with the values of the mixing parameter δ of the first transition of each cascade.
The sign of δ is chosen in accordance with ref. [36]). The resulting coefficients A_2 and

A_4 are listed in table 4 together with the deduced spin values. In further columns of this table the mixing parameters δ and the multipole admixtures

$$Q = \delta^2/(1+\delta^2)$$

are summarized.

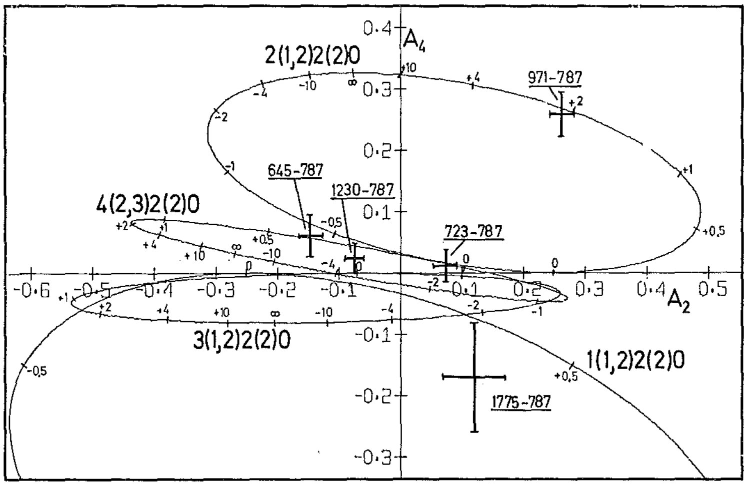

Fig. 5. Parametric plot of the angular correlation coefficients A_2 and A_4 for $J-2-0$ cascades ($J = 1, 2, 3, 4$). The ellipses are labelled with the values of the mixing ratio δ for the first transition. The experimental A_2, A_4 pairs are represented as crosses of error bars.

4. Discussion of the energy levels

A comparison of the present results with the levels of ^{98}Mo as observed in other nuclear reactions and in decay studies is given in table 5. Our energy values are in excellent agreement with those of ref. [18]). Below 1.8 MeV, in almost all investigations five levels are found at 735, 787, 1432, 1510 and 1759 keV. None of the levels observed in different studies between 1.8 MeV and 2.0 MeV (at 1812, 1881, 1930, 1965 and 1985 keV) could be confirmed by any other investigation. Above 2 MeV 15 of the 23 states found in the (n, γ) reaction may be identified with levels from at least one former publication, while the residual eight states were previously unknown.

The following remarks on the levels seem to be useful.

The ground state. No primary transition to the ground state has been observed. The intensity is expected to be small, since the multipolarity should be E2.

The 735 keV *level.* Of great interest is the appearance of a low-lying $J^\pi = 0^+$ level at 735 keV which has first been observed in ref. [1]). The weak primary transition at 7907 keV populating this level must have multipolarity E2. According to the angular momentum selection rule no de-exciting γ-ray at 735 keV is observed. The

TABLE 4

Results of the angular correlation measurements in ^{98}Mo

Cascade (keV)	Determined coefficients		Spin sequence J_i-J-J_f	Spin/parity assignment		Mixing ratio		
	A_2	A_4		level (keV)	J^{π}	transition (keV)	δ [a]	Q [a] (%)
645–787	-0.147 ± 0.020	0.060 ± 0.035	2–2–0	1432	2^+	645	-0.58 ± 0.05	25 ± 3
723–787	0.075 ± 0.018	0.012 ± 0.025	4–2–0	1510	4^+	723	0.04 ± 0.03	$0.20^{+0.30}_{-0.19}$
971–787	0.263 ± 0.020	0.261 ± 0.036	2–2–0	1759	2^+	971	2.15 ± 0.15	82 ± 2
1230–787	-0.074 ± 0.015	0.024 ± 0.025	3–2–0	2017	3^-	1230	0.00 ± 0.02	0.00 ± 0.04
1775–787	0.12 ± 0.05	-0.17 ± 0.09	1–2–0	2562	(1) [b]	1775	$0.36^{+0.03}_{-0.04}$	$11.5^{+2.0}_{-2.5}$

[a]) $\delta = \langle J||L+1||J_i\rangle / \langle J||L||J_i\rangle$; $Q = \delta^2/(1+\delta^2)$; choice of the sign of δ according to ref. [36]).

[b]) Cf. discussion in sect. 4.

transition to the ground state is accomplished 100 % by internal conversion and the half-life of this level has been determined to be 22 ± 1 nsec [ref. [1])].

The 787 keV *level.* The assignment $J^\pi = 2^+$ to this level is confirmed by (α, α') excitation [3]) and forms the basis of our angular correlation analysis.

The 1432 keV *level.* The angular correlation coefficients measured for the 645-787 keV cascade are consistent with the spin sequences 2-2-0 and 4-2-0. The sequence 4-2-0 is less probable in view of the resulting high octupole content. In addition spin $J = 4$ is excluded because of the strong 1432 keV ground state transition. The assignment $J^\pi = 2^+$ is in good agreement with refs. [18,20]). A weak previously unknown 698 keV transition has been observed proceeding to the $J^\pi = 0^+$ state at 735 keV.

The 1510 keV *level.* In view of the angular correlation of the 723-787 keV cascade the spin values $J = 2$, 3 or 4 are possible for the 1510 keV level. The assignment $J^\pi = 4^+$ given in fig. 4 has been adopted from refs. [18,20]). As expected the M3 admixture to the E2 transition at 723 keV is very small ($\delta = 0.04 \pm 0.03$). The attribution of spin 4^+ is supported by systematics and the analogy to ^{96}Mo.

The 1759 keV *level.* The angular correlation coefficients of the 971-787 keV cascade clearly reveal the spin sequence 2-2-0. The quadrupole admixture of the 971 keV transition amounts to 82 % and favours positive parity for the 1759 keV level. All de-excitations from this level are in good agreement with ref. [18]).

The 1881 keV *level.* The 6761 keV primary γ-ray and the 1093 keV and 449 keV secondary transitions establish a new level at 1881 keV. Assuming M1 radiation for the weak primary transition which is reasonable on the basis of intensity considerations the spin and parity values $J^\pi = 1^+, 2^+, 3^+$, and 4^+ are possible for this level.

The 2018 keV *level.* With the values taken from the literature [37]) for the radiation width $\Gamma_\gamma = 127$ meV and for the mean distance of the levels contributing to the radiation $D = 89$ eV the radiation strength

$$k = \frac{\Gamma_\gamma I_\gamma}{E_\gamma^3 A^{\frac{2}{3}} D}$$

of the 6625 keV transition is determined to $k_{6625} = 234 \cdot 10^{-10}\ \text{MeV}^{-3}$. This strength clearly exceeds the limit of about $30 \cdot 10^{-10}\ \text{MeV}^{-3}$ found for M1 radiation of nuclei in the mass region $20 < A < 180$ [fig. 3 in ref. [38])]. The resulting E1 character of the 6625 keV transition yields negative parity for the 2018 keV level. The angular correlation of the 1230–787 keV cascade limits the spin sequences to 3-2-0 and 4-2-0. Because of the 2017 keV ground state transition observed in coincidence with the 6625 keV γ-ray spin 4 may be excluded. The 2017 keV transition must be E3 radiation.

The 2105 keV *level.* Since de-excitations from this level to states with $J^\pi = 0^+$ as well as with $J^\pi = 4^+$ have been found, the assignment $J^\pi = 2^+$ to the 2105 keV level is very probable. In β-decay only two de-exciting γ-rays at 1317 keV and 673 keV have been observed [19]). The (n, γ) reaction reveals two additional weak transitions at 1370 keV and at 595 keV.

TABLE 5

Energy levels of ^{98}Mo observed in nuclear reactions and decay studies

(n, γ) [a] E (keV)	J^{π}	(d, p) [b] E (keV)	(d, d′) [c] E (keV)	J^{π}	β-decay [d] E (keV)	J^{π}	β-decay [e] E (keV)	J^{π}	(n, n′γ) [f] E (keV)
734.9 ±0.3	0^+	736±20			734.9	0^+	736	0^+	
787.42±0.1	2^+	787±15	790	2^+	787.5	2^+	787	2^+	788
1432.32±0.1	2^+	1435±15			1432.3	2^+	1432	2^+	1433
1510.13±0.1	4^+	(1513±15)			1510.1	4^+	1509	4^+	1510
1758.5 ±0.2	2^+	1761±15	1760		1758.8	2^+	1761	$(1, 2^+)$	1760
									1812 [g]
1880.9 ±0.3									
			1930						
									1965
					1985.1				
2017.61±0.1	3^-	(2025±15)	2040	3^-	2018.0				2020
									2039
2104.9 ±0.2	2^+	(2110±30)							2106
			2180						
2206.9 ±0.2	1, 2	2216±15			2207.2				2208
2224.0 ±0.2	$3(^+), 4^+$				2223.8		2223		
2333.4 ±0.2	$3(^+), 4^+$				2333.6				2334
2343.7 ±0.2		2340±20	2360		2343.7		2342		
2419.8 ±0.2	$3^{\pm}, 4^+$	2430±15			2419.9				
2485.4 ±0.2	$2^+, 3(^+), 4^+$								
2506.3 ±0.2		2530±25			2506.2				
2562.3 ±0.2	(1)								
2572.9 ±0.2		2585±15							
					(2608.5)				

[illegible] ±0.4				
2767.7 ±0.4	$3^{\pm}, 4^{+}$		2767.9	2767
2795.6 ±0.3				
		2829±20		
		2880±20		
		2925±20		
2962.4 ±0.3	$3^{-}, 4^{-}$			
2977.1 ±0.4		2980±30		
			3022.2	(3020)
3045.9 ±0.4				
		3066±15		
3103.1 ±0.5				
3108.8 ±0.3		3124±20		
3155.5 ±0.4		3168±20		
3195.5 ±0.5				
3210.7 ±0.4				
			3212.0	3210
		3270±30		
		3340±20		
			3395.2	
		3430±20		
			3455.5	(3455)
		3512±20	3502.8	
		3570±15		
		3636±20		
		3695±20		
		3740±30		
		3790±30		

[a]) This work. [b]) Ref. [9]). [c]) Ref. [2]). [d]) Ref. [18]). [e]) Ref. [20]). [f]) Ref. [11]). [g]) Probably due to a wrong placement of the 1024 keV transition.

The 2207 keV *level.* Considering the population of the 2207 keV level in the decay of the short-lived ^{98}Nb isomer [18]) the spin value may be limited to $J = 1$ or 2. In accordance with ref. [18]) only one secondary γ-ray at 1419 keV has been found.

The 2224 keV *level.* Because of the population of the 2224 keV level in the β-decay of 52 min ^{98}Nb [refs. [18,20])] and the direct feeding from the capture state in the (n, γ) reaction the spin value is very probably $J = 3$ or 4. In the case of $J = 4$ the parity must be positive in view of the 1437 keV and 792 keV transitions leading to levels with $J^\pi = 2^+$. If the spin is 3, positive parity is more probable than negative parity considering the small radiation strength of the primary transition. All transitions observed agree with those given in refs. [18,20]).

The 2333 keV *level.* The level at 2333 keV was first reported in ref. [18]) and later on confirmed in a publication [11]) on the (n, n'γ) reaction. Analogous to the preceding level at 2224 keV the spin and parity assignment may be limited to $J^\pi = 3^{(+)}$ or 4^+. In addition to the previously known secondary transitions with energies 1546 and 823 keV [ref. [18])] transitions to the 2^+ levels at 1432 keV and 1759 keV have been found in the present study.

The 2344 keV *level.* The level at 2344 keV which is populated in the decay of ^{98g}Nb only via γ-cascades [18,20]) is de-excited by the 834 keV transition observed in coincidence with the strong 723 keV γ-ray. The fact that this level is depopulated only to a level with $J^\pi = 4^+$ without primary feeding from the capture state may be explained by a spin value $J > 4$.

The 2420 keV *level.* With the same arguments used for the 2224 keV level the spin value of the 2420 keV level may be restricted to $J = 3$ or 4, in the latter case presumably with positive parity. Besides the well-known 910 keV transition [18]) further de-excitations have been found at 998, 662, 402 and 315 keV. Possibly the 1633 keV γ-ray observed in the β-decay [18]) is identical with the line no. 124 at 1631 keV in the present study. The energy precision achieved in the (n, γ) reaction, however, does not permit interpreting this line as a transition to the 787 keV level as has been done in ref. [18]). The level difference exceeds the γ-ray energy by about 1 keV which is well outside the experimental errors.

The 2485 keV *level.* According to the observed pattern of transitions which proceed to levels both with $J^\pi = 2^+$ and 4^+, spin and parity of the 2485 keV level may be limited to 2^+, $3^{(+)}$ or 4^+.

The 2506 keV *level.* The 173 keV γ-ray de-exciting the 2506 keV level has been observed in coincidence with the 823 keV transition also in the β-decay of ^{98g}Nb [ref. [18])]. Since the 996 keV γ-ray did not appear in the spectrum coincident with the 173 keV transition, this γ-ray has not been placed between the levels at 3503 keV and 2506 keV [ref. [18])], but between the levels at 2506 keV and 1510 keV.

The 2562 keV *level.* The angular correlation analysis yields spin $J = 1$ for the 2562 keV level (cf. table 4). It should be noticed, however, that no corrections for admixtures of the unknown angular correlation of the 1785–787 keV cascade have been made. Such admixtures may have falsified the angular correlation coefficients of the 1775–787 keV cascade. The assignment of spin 1 has therefore to be considered as somewhat tentative. On the other hand, $J = 1$ is consistent with the observation that this level is not fed in the β-decay from the $J^{\pi} = 4^-$ or 5^- ground state of ^{98}Nb [refs. [18,20])].

The 2621 keV *level.* From the 2621 keV level transitions to both the $J^{\pi} = 0^+$ state at 735 keV and to the $J^{\pi} = 4^+$ state at 1510 keV are observed. If the multipolarities are restricted to quadrupole radiation, the resulting spin value is $J = 2$ and the parity will be positive which is consistent with the radiation strength of the primary transition from the capture state. Energetically this level corresponds to a 2.63 MeV state found in the (d, p) reaction [9]) (see table 5).

The 2768 keV *level.* Due to the population of this level in the ^{98g}Nb β-decay and the direct feeding from the capture state the spin assignment of the 2768 keV level may be restricted to $J = 3$ or 4. In the case $J = 4$ the parity must be even, since the level is preferably de-excited to the 2^+ state at 787 keV. Besides the γ-rays at 1980 keV and at 435 keV observed in the (n, γ) reaction, further transitions at 1336 keV and at 1258 keV have been found in the β-decay of ^{98g}Nb [refs. [18,20])].

The 2796 keV *level.* Similar to the 2344 keV level a spin value $J > 4$ may provide an explanation both for the failure to detect a primary feeding of the 2796 keV level and for the absence of secondary transitions to levels with spin $J < 4$. However the fairly strong intensity of the 1285 keV γ-ray and the fact that this level is not observed in the ^{98g}Nb β-decay throw some doubt on such a high spin value.

The 2962 keV *level.* The radiation strength † $k = 37 \cdot 10^{-10}$ MeV^{-3} of the 5680 keV primary transition just exceeds the upmost limit for M1 radiation [38]). Therefore this primary transition has probably E1 character and the parity of the 2962 keV level is negative. In view of the 1452 keV and 945 keV transitions proceeding to levels with $J^{\pi} = 4^+$ and 3^- the spin value of the 2962 keV level is $J = 3$ or 4.

The 3211 keV *level.* The de-excitation mechanism of the 3210.7 keV level deviates considerably from that of the 3212.0 keV level reported by Herzog *et al.* [18]). The intensity ratio $I_{1701.9}/I_{1194.0}$ found by these authors in the β-decay is about 10 times greater than that observed in the (n, γ) reaction. Our energy value of the 3211 keV level is supported by the good fit of primary feeding from the capture state, and the precision achieved in our work does not admit placing the 1701.8 keV transition as a de-excitation to the 1510 keV level. An explanation of this discrepancy may be the existence of two closely spaced levels at 3211 and 3212 keV, the lower one with the de-excitation as given in fig. 4, the upper one [as reported in ref. [18])] with the 1701.9 keV and a weak 1194.0 keV transition, which is covered in the (n, γ) spectrum by the stronger 1193.3 keV line.

5. Comparison with nuclear models

^{98}Mo exceeds the nucleon number of ^{90}Zr by two protons and six neutrons. The configuration of ^{90}Zr is believed to be a suitable core for shell-model calculations[39–41])

† See the 2018 keV level.

When computing the molybdenum level schemes in such calculations the nucleons outside the ^{90}Zr core have been placed in the proton $\pi 1g_{\frac{9}{2}}$ orbit and the neutron $\nu 2d_{\frac{5}{2}}$ orbit. In ^{98}Mo this $\nu 2d_{\frac{5}{2}}$ orbit is totally filled up with the consequence that only proton excitation in the $\pi 1g_{\frac{9}{2}}$ orbit is possible at lower excitation energies. Therefore the level scheme of ^{98}Mo should resemble that of ^{92}Mo with a level sequence of 0^+ (ground state), $2^+, 4^+, 6^+, 8^+$ [ref. [40]]. However, this is not observed. The reason may be the inadequacy of restricting the neutrons to the $\nu 2d_{\frac{5}{2}}$ orbit. Experimental evidence of violation of this limitation is deduced from the (d, p) and (d, t) reactions [10]) which

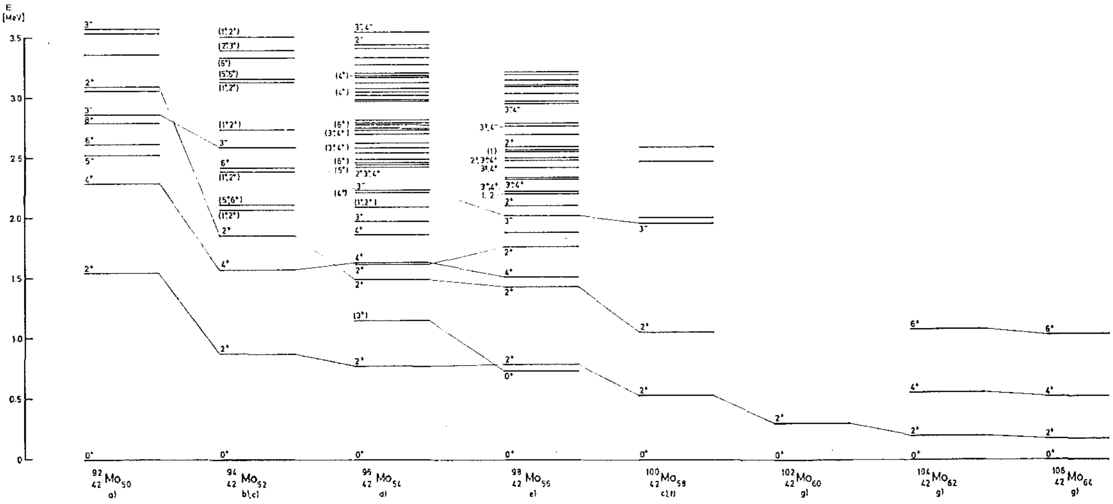

Fig. 6. The experimental level schemes of the stable even molybdenum isotopes. a) ref. [44]), b) ref. [45]), c) ref. [2]), d) ref. [32]), e) this work, f) ref. [6]), ref. [50]).

demonstrate that only 55 % of the neutrons beyond $N = 50$ may be found in the $\nu 2d_{\frac{5}{2}}$ orbit, 25 % occupy the $\nu 1g_{\frac{7}{2}}$ orbit, the rest is spread out on the $\nu 2d_{\frac{3}{2}}$ and $\nu 3s_{\frac{1}{2}}$ orbits.

Of special interest is of course the occurrence of the low-lying $J^\pi = 0^+$ level at 735 keV. In ^{90}Zr the first excited state at about 1.75 MeV is observed to be also a $J^\pi = 0^+$ level [42]). Its occurrence is assigned to a proton configuration composed of 37 % $(2p_{\frac{1}{2}})^2$ and 63 % $(1g_{\frac{9}{2}})^2$ [ref. [43])]. In ^{98}Mo with 42 protons two similar orthogonal configurations of

$$a(2p_{\frac{1}{2}})^2(1g_{\frac{9}{2}})^2 \pm b(2p_{\frac{1}{2}})^{-2}(1g_{\frac{9}{2}})^4$$

with $a^2+b^2 = 1$ may be responsible for the ground state and first excited state. If this assumption holds, then in the neighbouring even molybdenum isotopes low-lying $J^\pi = 0^+$ levels should exist, too. Possibly, in ^{96}Mo the second excited state at 1148 keV may be identified with this prediction [32]). In all other molybdenum isotopes such a level has not been observed till now as shown in fig. 6. In particular in ^{92}Mo with the closed $N = 50$ neutron shell where the levels should be ascribed predominantly to a proton excitation, no low-lying $J^\pi = 0^+$ level is found [44]). The ^{98}Mo(p, p') reaction [12]) yields that the excited state at 735 keV can not be interpreted by a simple shell-model configuration. An investigation of the ^{98}Mo(p, p'e$^-$) reaction [13]) points to a more complex nucleonic structure of this $J^\pi = 0^+$ level.

Another approach to the description of the excited levels in ^{98}Mo comes from the vibrational model. The 2018 keV level may very well be interpreted as the first octupole state and there exists, as expected in the vibrational model, a strong E3 transition to the ground state. In the harmonic approximation for the quadrupole states there is above the first 2^+ state a triplet with $J^\pi = 0^+, 2^+$, and 4^+ at twice the energy of the first 2^+ state. A comparison with the experimental level scheme leads to the identification of the 787 keV level with the first quadrupole vibrational state. An obvious member of the two-phonon triplet is only provided by the $J^\pi = 4^+$ state at 1510 keV. A decision on which of the two 2^+ states at 1432 keV and at 1759 keV has to be assigned to the two-phonon triplet may be obtained from the ratio of the reduced transition probabilities $b = B(\mathrm{E2}, 2^{+\prime} \rightarrow 2^+)/B(\mathrm{E2}, 2^{+\prime} \rightarrow 0^+)$. The corresponding values as determined in the present study are

$$b_{1432} = 16.0 \pm 2.1,$$

$$b_{1759} = 177 \pm 60 ,$$

which favours the 1759 keV level as a candidate for a two-phonon state. There is a remarkable similarity with the corresponding values for the 1498 keV level ($b = 15.7 \pm 2.5$) and 1626 keV level ($b = 145 \pm 22$) of the neighbouring ^{96}Mo isotope [32]). In fig. 6 the connecting lines between the level schemes give expression to this correspondence.

Completion of the two-phonon triplet by the first $J^\pi = 0^+$ state at 735 keV will bring problems because of the very large splitting of the triplet and because of the strong $\Delta N = 0$ transition between the levels at 1759 keV and 735 keV. Such a transition is forbidden in the harmonic approximation.

Sakai [46]) suggested interpreting the 0^+ and 2^+ states of the two-phonon triplet as the band heads of β- and γ-vibrational bands. This interpretation seems to be very attractive since there is ample evidence [47]) that the Mo isotopes with $100 < A < 110$ may have deformed equilibrium shape. The tendency of increasing deformability with increasing mass number is well illustrated by fig. 6. Experimental support is provided by the fact that γ-rays emitted from neutron-rich fission fragments in this mass region seem to follow rotational energy systematics [48-50]).

Therefore the level scheme of ^{98}Mo may be discussed in the framework of a newer collective model [51]). This model is very well suited in the transition region between spherical and deformed nuclei, because it describes all kinds of nuclei – spherical with harmonic and anharmonic vibrations as well as strongly deformed symmetric and asymmetric rotators – in a uniform manner. The potential energy which is a function of the deformation parameter β and the shape parameter γ

completely describes the nuclear surface and its collective excitations. For illustration the excited states of ^{98}Mo in the lower energy region have been collected into different bands, as shown in fig. 7. The relationship of the band states to the vibrational states (drawn in the middle of fig. 7) is indicated by dashed lines. In spite of the lack of information on the spin values of the higher energy levels, the existence of the various bands may be deduced by comparison with the states of the neighbouring ^{96}Mo isotope, which are displayed in fig. 7, too. Members of the ground state band will be the first $J^{\pi} = 2^{+}$ level at 787 keV and the first $J^{\pi} = 4^{+}$ level at 1510 keV. The next

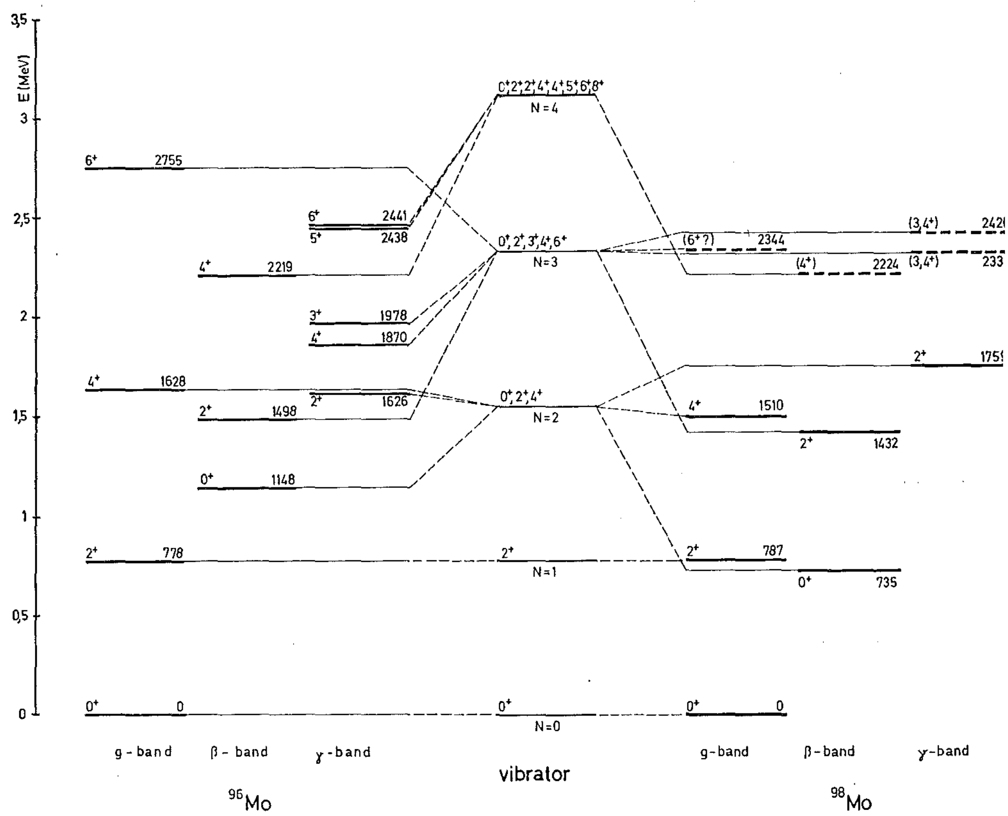

Fig. 7. Splitting of the ^{96}Mo [ref. [32]] and ^{98}Mo levels into band states. In the middle the (degenerated) states of the harmonic vibrator are shown. The relationship of the band states with the vibrational states is indicated by dashed lines. All energies are given in keV.

member of this band has spin $J = 6$. If such a level is populated in the (n, γ) reaction it may be identified with the 2344 keV level which is supposed to have $J > 4$.

The band head of the β-band with $J^{\pi} = 0^{+}$ is placed at 735 keV below the first 2^{+} level. Such a low-lying 0^{+} level may be generated by a potential energy surface in the $\beta\gamma$ plane which has a secondary minimum with a depth comparable to that of the main minimum near the spherical shape ($\beta \approx 0$). Besides this shape there exists another energy surface which also produces a low-lying 0^+ state: In a larger region around the spherical center the potential energy should be constant and independent of β and γ. Outside this region the energy should rapidly increase to infinity. In the case of such a square well potential the first 0^+ state comes down to 0.85 times the energy of the first 2^+ state [52]. In ^{98}Mo the 0^+ level is positioned at 0.93 of this energy.

The second member of the β-band is the $J^\pi = 2^+$ level at 1432 keV and if the assignment $J^\pi = 4^+$ is correct, the 2224 keV level may be the third state of this band.

The 2^+ level at 1759 keV may be regarded in this picture as the band head of the γ-vibrational band. The next members of this band have the spin values $J = 3$ and 4. According to their origin from the same vibrational multiplet they should be placed close together, possibly with interchanged spin sequence [see fig. 1 in ref. [51]]. Identification with two of the states at 2333 keV, 2420 keV or 2485 keV is reasonable, if the interpretation of the 2224 keV level is assumed to be correct. Thus below 2 MeV all states except the 1881 keV level may be interpreted in the framework of the band structure model.

The energy spacing within the bands does not obey the simple formula $E = J(J+1)\hbar^2/2\theta$ which is well fulfilled in the case of unperturbed rotational motion. This demonstrates that the ^{98}Mo nucleus is not a good rotational nucleus. On the other hand, the insufficiency of the vibrational model shows that ^{98}Mo may be regarded as a representative nucleus for the transitional region between vibrating spherical and rotating deformed nuclei. The excited levels can be understood qualitatively in the collective model of Gneuss *et al.* [51]. Quantitative predictions concerning level energies and transition intensities are still missing. Such data will allow a more rigorous check of the validity of the model.

References

1) K. Hübenthal, J. Berthier, J. C. Hocquenghem and A. Moussa, Compt. Rend. **265B** (1967) 162
2) Y. S. Kim and B. L. Cohen, Phys. Rev. **142** (1966) 788
3) N. P. Heydenburg and G. M. Temmer, Phys. Rev. **99** (1955) 617
4) G. M. Temmer and N. P. Heydenburg, Phys. Rev. **104** (1956) 967
5) P. H. Stelson and F. K. McGowan, Phys. Rev. **110** (1958) 489
6) Y. P. Gangrskii and I. K. Lemberg, ZhETF (USSR) **42** (1962) 1027; JETP (Sov. Phys.) **15** (1962) 711; Bull. Acad. Sci. USSR (phys.ser.) **26** (1962) 1009
7) R. L. Robinson, P. H. Stelson, F. K. McGowan, J. L. C. Ford, Jr. and W. T. Milner, Nucl. Phys. **74** (1964) 281
8) C. F. Moore, P. Richard, C. E. Watson, D. Robson and J. D. Fox, Phys. Rev. **141** (1966) 1166
9) K. R. Evans, F. Ajzenberg-Selove and B. Rosner, Phys. Rev. **165** (1968) 1327
10) S. A. Hjorth and B. L. Cohen, Phys. Rev. **135** (1964) B920
11) K. C. Chung, K. Swartz, A. Mittler, C. Robertson, T. D. Brandenberger and M. T. McEllistrem, Bull. Am. Phys. Soc. **14** (1969) 1238
12) J. J. Kent, C. F. Moore and C. E. Watson, Phys. Rev. **C1** (1970) 346
13) W. J. Courtney and C. F. Moore, Phys. Lett. **31B** (1970) 131
14) C. J. Orth and R. K. Smith, J. Inorg. Nucl. Chem. **15** (1960) 4
15) S. C. Gujrathi and S. K. Mukherjee, Nucl. Phys. **85** (1966) 288
16) K. Hübenthal, E. Monnand and A. Moussa, Compt. Rend. **264B** (1967) 1317
17) K. Hübenthal, Compt. Rend. **264B** (1967) 1468

18) W. Herzog, N. Trautmann, R. Denig and G. Herrmann, Frühjahrstagung der Deutsch. Phys. Ges. (Fachausschuß Kernphysik) Freudenstadt, 24. – 28.3.1969
19) W. Herzog, private communication
20) K. Hübenthal, E. Monnand and A. Moussa, Nucl. Phys. **A128** (1969) 577
21) E. D. Earle and S. Monaro, AECL **2639** (1966)
22) E. D. Earle and S. Monaro, private communication cited in: G. A. Bartholomew, A. Doveika, K. M. Eastwood, S. Monaro, L. V. Groshev, A. M. Demidov, V. I. Pelekhov and L. L. Sokolovskii, Nucl. Data **A3** (1967) 601
23) D. Heck, W. Michaelis, H. Ottmar and H. Schmidt, Proc. on neutron capture gamma-ray spectroscopy (IAEA, Vienna, 1969) p. 309
24) G. A. Bartholomew, A. Doveika, K. M. Eastwood, S. Monaro, L. V. Groshev, A. M. Demidov, V. I. Pelekhov and L. L. Sokolovskii, Nucl. Data **A3** (1967) 373
25) U. Fanger, D. Heck, W. Michaelis, H. Ottmar, H. Schmidt and R. Gaeta, Nucl. Phys. **A146** (1970) 549
26) W. Michaelis and H. Küpfer, Nucl. Instr. **56** (1967) 181
27) U. Fanger, Thesis University Karlsruhe (1968); KFK **887** (1969)
28) H. Schmidt and D. Heck, Proc. on neutron capture gamma-ray spectroscopy (IAEA, Vienna, 1969) p. 371
29) H. Schmidt, KFK 877 (1970)
30) G. Krüger, G. Dimmler, G. Zipf, H. Hanak and R. Merkel, Kerntechnik **8** (1966) 273
31) G. Krüger, Proc. on Teilnehmer-Rechensysteme (Oldenbourg-Verlag, Munich and Vienna, 1968) 135
32) D. Heck, N. Ahmed, U. Fanger, W. Michaelis, H. Ottmar and H. Schmidt, Nucl. Phys. **A159** (1970) 49
33) L. V. Groshev, A. M. Demidov, V. I. Pelekhov, AEC-tr-**4685** (1960); Nucl. Sci. Abstr. **16** (1962) 108, abstr. 1032
34) D. Heck, KFK **1247** (1970)
35) J. H. E. Mattauch, W. Thiele and A. H. Wapstra, Nucl. Phys. **67** (1965) 32
36) L. C. Biedenharn and M. E. Rose, Rev. Mod. Phys. **25** (1953) 729
37) H. Shwe and R. E. Coté, Phys. Rev. **179** (1969) 1148
38) G. A. Bartholomew, Ann. Rev. Nucl. Sci. **11** (1961) 259
39) I. Talmi and I. Unna, Nucl. Phys. **19** (1960) 225
40) J. Vervier, Nucl. Phys. **75** (1966) 17
41) K. H. Bhatt and J. B. Ball, Nucl. Phys. **63** (1965) 286
42) O. E. Johnson, R. G. Johnson and L. M. Langer, Phys. Rev. **98** (1955) 1517
43) B. F. Baymann, A. S. Reiner and R. K. Sheline; Phys. Rev. **115** (1959) 1627
44) K. Lieb, T. Hausmann and J. J. Kent, Phys. Rev. **182** (1969) 1341
45) J. Barette, A. Boutard and S. Monaro, Can. J. Phys. **47** (1969) 995
46) M. Sakai, Nucl. Phys. **A104** (1968) 301
47) S. A. E. Johansson, Nucl. Phys. **64** (1965) 147
48) F. Horsch and W. Michaelis, Proc. on physics and chemistry of fission (IAEA, Vienna, 1969) p. 527;
F. Horsch, Thesis University Karlsruhe (1970)
49) G. Zicha, K. E. G. Löbner, P. Maier-Komor, J. Maul and P. Kienle, Contrib. Int. Conf. on properties of nuclear states, Montreal, Canada (Les Presses de l'Université de Montreal, 1969) p. 83
50) E. Cheifetz, R. C. Jared, S. G. Thompson and J. B. Wilhelmy, Phys. Rev. Lett. **25** (1970) 38
51) G. Gneuss, U. Mosel and W. Greiner, Phys. Lett. **31B** (1970) 269
52) A. Kamlah, private communication